Radiocaesium sorption on natural glauconite sands is unexpectedly as strong as on Boom Clay

Y. Bruneel[1,2] , L. Van Laer[1], S. Brassinnes[3], E. Smolders[2]

[1] Belgian Nuclear Research Centre (SCK•CEN), Expert Group Waste & Disposal, Boeretang 200, 2400 Mol, Belgium

[2] Department of Earth and Environmental Sciences, Division of Soil and Water Management, KU Leuven, Kasteelpark Arenberg 20, 3001 Leuven, Belgium

[3] ONDRAF/NIRAS, the Belgian Agency for Radioactive Waste and Fissile Materials, Kunstlaan 14, 1210 Brussel, Belgium

E-mail: ***yaana.bruneel@sckcen.be***

Abstract

The Neogene-Paleogene glauconite sands of Belgium cover the Boom Clay deposits that are candidate host for radioactive waste disposal. It is unclear if the highly permeable sand formations may act as an additional barrier for radiocesium (^{137}Cs) or could be added as a complementary sorption sink in a surface disposal concept. Glauconite is an Fe-rich phyllosilicate that is mainly present as 250-125 µm sized pellets in sand, it is unknown to what extent and how fast these pellets may bind ^{137}Cs. Pelletized clays embedded in sand may have poorly accessible high affinity sites for ^{137}Cs. The ^{137}Cs sorption on 11 different glauconite sands was measured in batch in a background solution of 0.1 M $CaCl_2$ and 0.5 mM KCl. The log transformed ^{137}Cs distribution coefficient K_d (L kg^{-1}) after 30 days reaction ranged 3.4-4.3, surprisingly close to the K_d of the Boom Clay (3.5). Isolated glauconite fractions exhibited similar ^{137}Cs sorption potentials (log K_d 4.1-4.3) as the reference Illite du Puy (4.4). The small K_d variation among the Neogene-Paleogene sands was explained by its glauconite content (r=0.82). The ^{137}Cs sorption kinetics (1-57 days) of milled pellets (<2 µm) confirmed slower reaction with intact pellets than with milled samples. Additionally, the K_d values of milled samples (57 days) sorption are 1.1-1.5 fold larger than the corresponding intact pellets, suggesting that not all Cs binding sites are accessible in intact pellets. Strongly weathered pellets exhibited cracks (visible with SEM). In these pellets the K_d was similar for milled and intact pellets suggesting that cracks increase the accessibility of the inner sorption sites. After 8.5 months the K_d values were 1.6-1.8-fold above corresponding 1 month data and these long-term reactions were more pronounced as total sand K content was larger. An adsorption-desorption experiment illustrated that ^{137}Cs sorption is not fully reversible.

Keywords

Neogene-Paleogene, Belgium, pelletal glauconite, kinetics, weathering, radioactive waste disposal

1 Introduction

Radioactive waste needs to be stored securely for hundreds to hundreds of thousands of years. Sand formations are generally not considered a suitable host material for radioactive waste repositories due to their high permeabilities and low sorption potentials. This implies fast transport of radionuclides (RN) with the pore water, against any potential disposal concept. In Belgium, the Neogene-Paleogene glauconite sands are, however, being considered as natural barrier. These sands are highly permeable, but contain a strongly sorbing component, glauconite. These Neogene-Paleogene glauconite sands may be added as an extra embankment below the surface disposal for the short-lived and low-level waste. For the high-level and/or long-lived radioactive waste, deep geological disposal is proposed. Host rocks that might qualify for long term disposal are poorly indurated clays 200 to 600 m below the surface (e.g. Boom Clay or Ypresian clays). Both Boom Clay and Ypresian clays are enclosed in glauconite-rich sands or silts. In the Neogene and Paleogene marine sands, glauconite is very abundant. Some formations have low percentages (5%), others have, on average 35-40% (e.g. Diest and Berchem Fm) and locally percentages up to 80% occur (Adriaens et al. 2014). In the NE of Belgium, the 100 m thick Boom Clay layer is situated below about 100 m of Neogene-Paleogene glauconite sands and above 175 m of Paleogene glauconite sands/silts.

Glauconite is a phyllosilicate, classified as a clay mineral, but mostly present as course pellets in the sand-silt fractions (2 – 0.002 mm), only minor amounts are found in the clay fraction (< 2µm). The term glauconite is often used for the description of green globular silt-to sand-sized pellets in sediments, without any mineralogical connotation. The mineral glauconite $(K,Na)(Fe^{3+}Fe^{2+},Al,Mg)_2(Si,Al)_4O_{10}(OH)_2$ is described as an iron (Fe) - potassium (K) phyllosilicate, comparable to an Fe-rich illite with K the main interlayer cation. Finding a pure glauconite is exceptional, most often glauconite pellets consist of one or more Fe-rich mixed layer glauconite-smectite phases (Meunier et al. 2007, Adriaens et al. 2014). In this work the term ‘glauconite’ refers to the green pelletal fraction of the sands, unless stated otherwise.

The diverse composition of glauconite pellets stems from both the formation and weathering history. Glauconite is formed through diagenesis of granular substrates in marine sediment at shallow depth. During formation K^+ and Fe are incorporated in the structure. The K^+ content increases with maturity with $K^+ > 8$ wt% for mature glauconite (Odin 1988, Meunier et al. 2007). Due to the presence of both Fe^{3+} and Fe^{2+}, glauconite is redox

sensitive. During weathering Fe and Mg are removed from the structure and K^+ is leached from the interlayer by which glauconite evolves to a more smectitic form (Courbe et al. 1981, Van Ranst et al. 1983). Additionally, physical weathering can cause the disintegration of the glauconite pellets to the clay fraction glauconite. The Neogene-Paleogene glauconite mineralogy has been studied in detail by Adriaens et al. (2014) for both pelletal and clay sized glauconite. On average, the glauconites have 6-12 % expandable layers and total Fe content of 16 – 23.5 wt% with Fe^{3+}/Fe^{2+} of 9/1. The high K content (5.5 – 7 wt% K_2O) makes the Neogene-Paleogene glauconites highly mature according to the classification of Odin (1988).

Sorption of RN on glauconite (sands) are not as widely studied as sorption on illite. This study focuses on the sorption of ^{137}Cs on glauconite sands. Caesium-137 poses a long term radiation risk due to a combination of a long half-life $t_{1/2}$ of 30 years and a large dose rate. Caesium is present in the environment as monovalent hydrated Cs^+ and is highly soluble under all E_h and pH conditions. The mobility of ^{137}Cs in the environment is mainly controlled by sorption on clay mineral surfaces in soils (Sawhney 1972, Takeno 2005, Fuller et al. 2015). Just as illite, glauconite is expected to have strong sorption, but the pellet form might be an obstacle for fast and near complete immobilization. The Cs sorption sites in glauconite are largely similar to the sites on illite due to the chemical and mineralogical resemblances between both minerals. This suggests a high sorption potential, however that sorption may be limited by slow intraparticle diffusion, i.e. slow or incomplete within realistic time frames.

The Cs^+ sorption on illite can be described by a three site exchange model: frayed edge sites (FES), type II sites and planar sites (Figure 1) (Poinssot et al. 1999, Bradbury & Baeyens 2000, Fuller et al. 2015). The frayed edge sites and type II sites are often considered together as the highly selective sites, with Cs-K selectivity coefficients exceeding 10^4. The FES have the highest specificity for Cs over other monovalent cations (e.g. K^+, NH_4^+, sodium (Na^+)) and are responsible for strong sorption of Cs in the low, but relevant, concentration domain. Larger ions simply do not fit in the limited space of the FES. Despite the high selectivity for Cs^+, the FES are only representing 0.25 % of the total CEC (cation exchange capacity) (Bradbury & Baeyens 2000). The type II sites can be found at the edges of the layers. Here, the layers are sufficiently widened to be accessible to larger ions reducing the selectivity for Cs^+. The planar sites originate from the isomorphic substitutions in the structure. The permanently negative charged surfaces provide high capacity but low affinity sites (Bradbury & Baeyens 2000). ^{137}Cs sorption on the planar sites of illite is fast, with only a few hours to reach equilibrium. On the frayed

edge sites sorption equilibrium is only reached after 4-5 days, most probably due to the size and the accessibility of the sites compared to the planar sites (Poinssot et al. 1999).

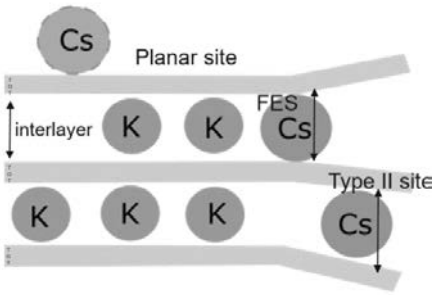

		FES	Type II sites	Planar sites
(Bradbury and Baeyens, 2000)	Capacity (meq kg^{-1})	0.5	40	160
	Log $^{Cs}_{K}K_c$	4.6	1.5	0.5
(Fuller et al., 2014)	Capacity (meq kg^{-1})	0.004	1.6	65
	Log $^{Cs}_{K}K_c$	5.5	3.0	1.1
(Missana et al., 2014)	Capacity (meq kg^{-1})	0.46	39	155
	Log $^{Cs}_{K}K_c$	4.2	2.0	1.15

Figure 1 Three site model with site capacities (meq kg^{-1}) and site selectivity coefficients (log K_c) for modelling Cs sorption on illite as described by three different authors (Bradbury & Baeyens (2000), Fuller et al. (2014), Missana et al. (2014)).

Potassium has a perfect size to fit in the interlayer and due to the positive charge the negative clay layers are attracted. Increasing the K^+ content causes a stronger 'bond' between the clay layers or a so called layer collapse. When K^+ is leached from the interlayer, due to weathering for example, the layer edges open up and new frayed edge sites are available to Cs sorption.

This study aimed to assess the sorption of trace ^{137}Cs ([Cs] < 10^{-7} M) on natural glauconite sands from the Neogene-Paleogene formations in Belgium. It is assumed that glauconite is the main sorbing component in the sands. The sorption of ^{137}Cs on glauconite is expected to be similar to ^{137}Cs sorption on illite for clay sized fractions, however, sorption might be slower or less complete for the pellet form due to restricted access to the inner sorption sites. In addition, the mineralogical and compositional variation in the glauconite sands among different formations is addressed, that mineralogy is expected to affect the ^{137}Cs sorption. A series of glauconite sands were sampled, their mineralogical compositions were characterized and ^{137}Cs sorption was measured with due attention to reaction kinetics. Pellet isolation and pellet grinding were used as experimental treatments to interpret sorption data of intact sands.

2 Materials and methods

2.1 Glauconite sands

2.1.1 Sample selection

All experiments were performed using natural glauconite sands. A selection of 11 sand samples was made over the Voort, Berchem and Diest Formation (Fm) from the Neogene-Paleogene layer above the Boom Clay in Mol (NE Belgium). These formations have variable glauconite and total clay mineral content. Some sections of the formations have been reworked or eroded, leading to variable weathering states in the glauconite pellets. Samples were collected from the drilling core ON-Dessel5 and the shaft excavation. Two reference samples, i.e. purified Na-conditioned Illite du Puy and a Boom Clay sample, were included (Table 1).

Table 1 Inventory of the selected glauconite sand samples from the Neogene-Paleogene formations for this study. The ON-Dessel5 31W370 borehole from the collection of NIRAS/ONDRAF was sampled at four positions to get a wider variability of samples in the section of Diest-Berchem Formation. The samples indicated with shaft excavation originate from the excavation of the second shaft to the underground lab HADES in Mol. The Boom Clay sample is a sample from a recent sampling campaign at HADES level. The sampling depth is expressed in mTAW, or the reference level in Belgium (Tweede Algemene Waterpassing).

	Formation	Member	Origin	mTAW	Lithology	sample fractions			
						Complete sample	Glauconite fraction	Milled complete sand	Milled glauconite fraction
D1	Diest		Shaft excavation	-73	Sand	X	X	X	X
D2	Diest		Shaft excavation	-91	Sand	X	X	X	X
D3	Diest		ON-Dessel 5-30	-95	Sand	X			
D4	Diest	Dessel	ON-Dessel 5-44	-109	Sand	X			
D5	Diest	Dessel	ON-Dessel 5-48	-113	Sand	X			
B1	Berchem	Antwerp	ON-Dessel 5-63	-126	Sand	X	X	X	X
B2	Berchem	Antwerp	Shaft excavation	-134	Sand	X		X	
B3	Berchem	Antwerp	Surface sand, Boom Clay quary Wienerberger Rumst	30.5	Sand		X		X
V1	Voort		Shaft excavation	-144	Clayey sand	X		X	
V2	Voort		Shaft excavation	-152	Clayey sand	X			
V3	Voort		Shaft excavation	-140	Clayey sand	X	X	X	
I	Na-illite du Puy		Reference material		Clay	X			
BC	Boom Clay	Putte	HADES sampling campaign 2017	-197	Clay	X			

2.1.2 In-situ pore water samples

Fresh in-situ pore water samples were sampled in several piezometers in the region to achieve porewater compositions in each formation. The piezometers (R-4b, L64a, L64b, R-4c and R-6d) were selected at corresponding depth and formation for the glauconite sand samples. Before sampling, the well volume was pumped out three times to get fresh aquifer water. The porewater samples were acidified in the field with 1% HNO_3.

2.1.3 Sample preparation

The samples had been stored after sampling in vacuum sealed bags under variable conditions, i.e. in a freezer or cooled room. Before use in the batch sorption experiments, the samples were dried at 60 °C. Part of the experiments were performed on the separated glauconite fraction of the samples; Table 1 shows the selected samples. Glauconite can be separated from the matrix by magnetic separation (Frantz Isodynamic magnetic separator). Since the glauconite fractions contain quartz-clay-iron oxide aggregates that are also attracted by the magnet, wet sieving was done to break these aggregates up. The sieving is also needed to improve the isolation of glauconite from the glauconite sand. The attraction of the glauconite grain to the magnet depends on the grain size. Using a narrower grain size fraction (125-250 µm) improves the separation of the glauconite grains from the sand. The quality of the separation was checked under the microscope and separation was repeated until a glauconite content of 99 % was reached in the glauconite fraction. Static minerals such as muscovite often pose a problem for the separation as they are also attracted by the electromagnet. For samples containing a lot of muscovite, the platelets were separated from the glauconite with a thin plastic sheet.

A subset of the glauconite fraction samples (Table 1) was milled to clay size with a McCrone Micronizing mill, a wet milling to avoid damage to the crystal structure (Środoń et al. 2001). This sample preparation resulted in four types of samples: complete glauconite sand, glauconite fraction (magnetically separated from the 125-250 µm fraction of the glauconite sand) a milled complete sand and a milled glauconite fraction.

2.2 Sample analysis

2.2.1 X-ray diffraction (XRD) analysis

Complete glauconite samples were milled (McCrone micronizing mill) to create fine random powders for XRD analysis. To the sample, 10 m% zincite was added as internal standard. QUANTA (© Chevron ETC) was used for data interpretation and quantitative data analysis. QUANTA is pattern summation software that uses the

concept of the Mineral Intensity Factor (MIF) to quantify the different mineral phases in a mixture. This concept attributes an intensity value to each mineral phase related to the stable reflection of the internal standard (zincite). For clay minerals the 060 peak position is typically used. However, this implies that clay minerals with a similar 060 peak position will be quantified together (e.g. glauconite, nontronite, Fe-smectite). To avoid an overestimation of the glauconite wt%, oriented clay slides were made to test for the presence of nontronite and smectite.

2.2.2 Cation exchange capacity - cobalt(III) hexamine chloride

The effective CEC was determined with the method as described in the standardised protocol ISO 23470 (2018) with adapted mass and volume of extractant. The cobalt (Co) complex is a stable trivalent cation that replaces the exchangeable cations on the negatively charged surfaces, i.e. the planar sites. This allows a one-step extraction with a 0.0166 M cobalt(III) hexamine chloride solution (Cohex) $[Co[NH_3]_6]Cl_3$. Measuring the CEC on natural glauconite samples is more complicated than in standard soils or clays. The pellet size implies that not all cation exchange sites might be (instantly) accessible for the large Co-complex. However, increasing the contact time might allow the Co to exchange some of the Fe. Therefore all samples were milled and the effective CEC can be referred to as the potential CEC. The effective CEC was determined by measuring the remaining Co concentration in solution after one hour of contact time by inductively coupled plasma mass spectrometry (Agilent Technologies 7700 Series ICP-MS).

2.2.3 Major element analysis

The major elements were determined in the porewater samples, glauconite sands and glauconite fractions. Fresh in-situ porewater samples were measured with ICP-MS (Agilent Technologies 7700 Series). The solid samples were prepared in duplicate with the lithium(Li)-metaborate fusion method of Vassilieva modified from Suhr et al. (1966) and Cremer et al. (1976). Samples were measured with the inductively coupled plasma optical emission spectroscopy (ICP-OES – Varian 720ES). A set of reference samples were chosen for data quality control, depending on the expected concentration of the major elements in the solution and additional elements of interest. In this case six reference samples were prepared with Li-metaborate and added to the batch for analysis (BCR-2, MRG-1, BCS-267, BCS-269, NIST-610, GA).

2.2.4 Fe^{2+} - Fe^{3+} speciation

The phenantroline method (Shapiro 1960, Fritz et al. 1985) was used to determine the Fe speciation in the glauconite fraction (performed in triplicate). In this method samples are dissolved in a HF and H_2SO_4 solution in

the presence of 1.10-phenantroline. The phenantroline forms a bright orange complex with Fe^{2+} and prevents further oxidation. To determine the Fe^{2+} content, the absorbance of the supernatants was measured at 555 nm using a Varian Model 635 UV-Visible Spectrometer. The total Fe content of the supernatants was determined by Atomic Absorption Spectroscopy (AAS) at 248 nm using a Thermo Electron Corporation S series AAS. The Fe^{2+} and Fe_{tot} mass percentages are calculated through a calibration curve obtained from geological Standard Reference Materials (SRM). A series of seven SRM's were selected based on the expected Fe^{2+} and Fe_{tot} content (NIM-G, GA, SY-3, DR-N, MRG1, BCR1 and NIM-D).

2.3 Batch sorption studies

The sorption is described by the distribution coefficient K_d (L kg^{-1}), i.e. the ratio of adsorbed to solution ^{137}Cs concentration, the former calculated from the difference in radiocaesium concentration in solution between initial and final samples. Due to the strong competition with K^+, ^{137}Cs sorption is often expressed as the radiocaesium interception potential (RIP or $K_d.m_K$) or the distribution coefficient independent of the K^+ concentration (de Preter 1990, Wauters et al. 1996). The inverse linear relation between the K_d and the K^+ concentration (m_K) makes it possible to recalculate sorption potential values to the in-situ K_d.

The ^{137}Cs sorption on glauconite sands was studied in a batch sorption test with a K-Ca background solution following the experimental procedure adapted from Wauters et al. (1996). The samples were prepared in duplicate and equilibrated in a background solution of 100 mM $CaCl_2$ and 0.5 mM KCl with a solid/liquid ratio of 1 g to 30 mL or 0.5 g to 80 mL. The relatively high Ca^{2+} concentrations are used to saturate the planar sites in order to study Cs sorption only at the specific sorption sites. Since the samples were pre-equilibrated in the K-Ca background solution, only the $^{137}Cs^+$ and K^+ can participate in ion exchange reaction on the FES. Sorption experiments were performed at neutral pH in a non-buffered system. The Cs sorption on glauconite at trace concentration levels is not pH dependent (Poinssot et al. 1999). Compared to standard batch sorption tests with illite (Comans et al. 1991, Voronina et al. 2015), the solid/liquid ratios in these batch sorption experiments are higher. Due to the large glauconite grains in the sand, larger solid sample sizes were required to have a representative sample.

The samples were weighed in dialysis bags (standard RC tubing, MWCO 6-8 kDa) and filled with 5 mL of background solution. Thereafter, they were transferred in 50 or 100 mL polypropylene (PP) tubes or bottles filled with 25 or 75 mL outer solution to obtain a solid/liquid ratio of 1 g to 30 mL or 0.5 g to 80 mL. This

dialysis tubing does not affect the sorption kinetics (Poinssot et al. 1999). The tubes were shaken on an orbital bench shaker (0.42 s^{-1}). After establishing equilibrium between sample and background solution (the outer solution is renewed four times with 8 to 16 hour time intervals), the solution was labelled with radiocaesium. The initial ^{137}Cs activity in the solution was 1.5 kBq mL^{-1} containing 0.01 µg mL^{-1} CsCl carrier and agitation continued. The evolution of the ^{137}Cs activity concentration in solution was measured (TriCarb 2100TR, Perkin Elmer Ins.) at different time intervals from 8 hours up to 8.5 months after initial spiking, thereby identifying kinetics in these large pellets. At each sampling point 1 mL of the supernatans (outer solution) was sampled and replaced by an equal volume of 0.5 mM K, 0.1 M Ca solution. In the calculation of the K_d, this dilution effect was taken into account. The equilibrium K concentrations were regularly measured by ICP-MS and were all within 6% of the nominal concentration of 0.5 mM.

An adsorption-desorption experiment was performed on a on a set of 10 complete glauconite sands and a subset of 4 milled samples. The samples were prepared with the same procedure as the batch sorption experiments. After 3 months of batch sorption, the membrane bags containing 1 g of soil and 5 mL of solution were placed in 25 mL ^{137}Cs free background solutions (0.5 mM K, 100 mM Ca). The ^{137}Cs activity concentrations in the outer solution were measured up to 7 days and activity data were corrected for the dilution with the inner solution.

3 Results and discussion

3.1 Glauconite sand and glauconite pellet properties

The glauconite sands are optically and mineralogically very different in terms of composition, grain size and grain morphology. The Diest Formation sands are coarse grained, contain 23-34 % glauconite and have very little to no other clays present. The range of globular to rounded glauconite pellets in these sands are associated with iron oxides on the outer rim and in the cracks of the grain. A crosscut of the grains shows a more oxidized outer rim (Figure 2). Pyrite is present in the inner part and in the cracks of some of the grains. The combination of oxidation rim and pyrite can be explained by formation in (locally) reducing conditions followed by a oxidation phase, probably during redeposition, and anoxic conditions after redeposition. In the lower Berchem and Voort Fm samples the visible signs of weathering (iron oxide rim, oxidized outer rim) are no longer present. These changes in mineralogy can be of importance as they can influence the sorption sites. Due to weathering, K

is leached from the interlayer and more edges open up. This can imply an increase in the amount of FES or it could lead to more FES being transformed to type II sites.

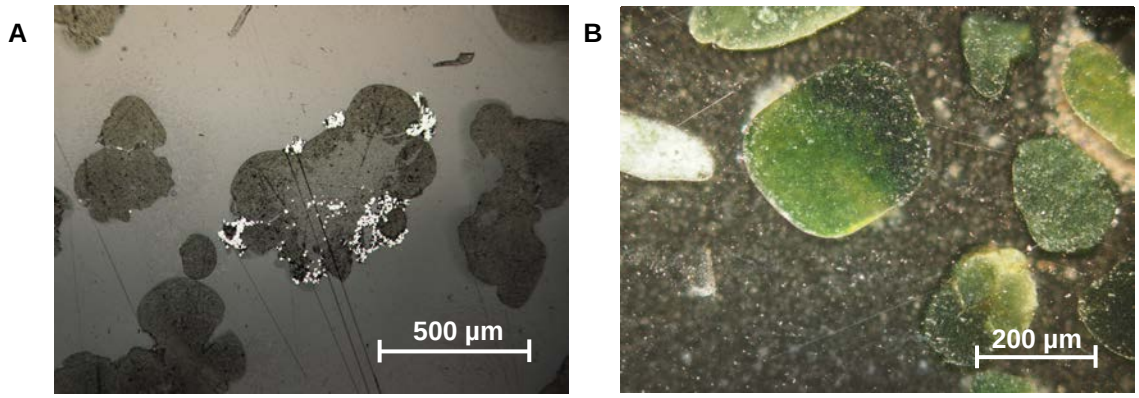

Figure 2 a) Crosscut of a globular glauconite pellet containing pyrite (white spots) both in the center and in the cracks (B2). b) Gradual color changes indicative of differences in K content in a rounded glauconite grain (D3).

The glauconite mineralogy is studied by three proxies: the K content, the Fe content and the cation exchange capacity (CEC) (Table 2). In theory, high K content implies mature glauconite (confer mature glauconite according to Odin (1988) 4-7 wt% K_2O) with low weathering grade. During weathering the structural Fe^{2+} can be oxidized to Fe^{3+} and the total Fe content in the glauconite can decrease due to Fe leaching from the structure, mostly combined with the formation of Fe-oxy-hydroxides. The complexity in these proxies is their relation to each other. Releasing K from the interlayer decreases the attraction of the interlayers and increases the accessible interlayer space, an effect visible in the CEC. All investigated glauconite fractions in the Neogene-Paleogene glauconite sands can be considered mature glauconite with a K_2O wt% of 5.8 – 8.3. For both the Fe content and CEC the inter and intra formation variation is similar. The Fe contents are between 25.6 -152 mg g^{-1} for the complete sands and 85-195 mg g^{-1} for the glauconite fractions. The CEC ranges between 8.20 – 17.4 $cmol_c$ kg^{-1}. Most of the investigated properties of complete glauconite sands are correlated, it is rather obvious that such structural properties are inherently interrelated (Table 4). Glauconite is the main Fe-K-Mg containing component in the sand, therefore the content of these elements in the sand depends on the glauconite content. Based on these data the formations cannot be distinguished.

Table 2 The range, mean values (arithmetic mean) and standard deviation (SD) of a series of analysis parameters for the glauconite sands described in Table 1.

	XRD			Phenantroline complexation	Major elements – complete sands			Major elements – glauconite fraction				
	Qz	GL	total clay	$\frac{Fe^{2+}}{Fe_{tot}}$	Fe	K	Mg	Fe	K	Mg	CEC sand	CEC glauconite fraction
		%				mg g^{-1}			mg g^{-1}			$cmol_c$ kg^{-1}
Min	8.0	8.0	26	0.169	25.6	14.2	4.4	85	28.6	10.8	8.20	26.8
Max	64	89	89	0.247	152	59.1	19.6	195	69.7	23.4	17.4	33.3
Mean	53	31	36	0.204	57.8	26.9	7.9	155	53.7	20.1	11.2	27.9
SD	15.4	22	19	0.028	36.8	11.9	4.2	31	11.2	3.67	2.46	2.91
D1	59	34	34		79.3	25.2	7.5	189	54.1	19.1	10.7	26.9
D2	60	27	31		58.8	23.2	6.9	155	47.9	18.4	8.20	24.2
D3	64	24	27	0.227	52.1	23.1	6.2	85	28.6	10.8	9.43	28.8
D4	64	23	26	0.247	43.2	23.2	6.1	141	53.6	20.3	9.52	
D5	57	30	33	0.183	26.6	14.2	4.4	148	58.3	23.4	12.0	30.1
B1	8.0	89	89	0.184	152	59.1	19.6	174	65.8	21.9	17.4	24.8
B2	56	27	32	0.216	49.2	28.5	7.3	195	69.7	23.0	11.3	33.3
V1	55	17	29		33.8	23.3	6.3	158	56.6	22.8	11.1	
V2	54	8.0	27		25.6	22.6	6.4	147	48.4	20.9	11.3	
V3	51	17	33	0.169							13.8	27.5

3.2 Cs sorption on glauconite sands

A preliminary test showed that the ^{137}Cs continued to react beyond the standard times used in the protocols of de Preter (1990) and Wauters et al. (1996) but that equilibrium was near completeness after about one month. Therefore, K_d data are first given for the apparent equilibrium at one month of interaction time. The log K_d values (L kg^{-1}) of the complete glauconite sands range from 3.36 to 4.25 at 0.5 mM K (Table 3). Surprisingly these values are in the same range as the value for the Boom Clay Formation (3.54). The K_d's are significantly different among sands and formations. The factor 5.7 difference in K_d's among sands is, however, small relative to that in surveys of corresponding studies in various soils where the K_d's range often beyond factor 200 (Waegeneers et al. 1999, Uematsu et al. 2015). The sand sample B1 with the highest glauconite content had also the highest K_d , in the range of the K_d of illite (reference sample Illite du Puy, Table 3).

Table 3 The log Kd (L kg-1) values of the complete glauconite sands after 35 days, means ± standard deviation of two replicates.

Formation	Sample	log K_d (L kg^{-1}) complete sand	Log K_d (L kg^{-1}) glauconite fraction
Diest Fm	D1	3.46 ± 0.02	4.14 ± 0.03
	D2	3.42 ± 0.03	4.16 ± 0.03
	D3	3.36 ± 0.01	
	D4	3.53 ± 0.01	
	D5	3.75 ± 0.03	
Berchem Fm	B1	4.25 ± 0.05	4.27 ± 0.01
	B2	3.59 ± 0.01	
	B3		4.09 ± 0.02
Voort Fm	V1	3.59 ± 0.02	
	V2	3.57 ± 0.03	
	V3	3.86 ± 0.01	4.26 ± 0.01
Illite du Puy	Ref	4.39 ± 0.05	
Boom Clay	Ref	3.54 ± 0.03	

Regression analysis is often used to link the sorption potential to soil properties. We aim to study the effect of mineralogical variations on the K_d and to evaluate if any of these parameters can be used to predict the sorption potential.

The interesting parameters are the CEC, the Fe and K content as they reflect the weathering state of the glauconite (Table 4). In the previous section we explained that the intra and inter formation variation for these parameters has a similar range. In the complete glauconite sands the glauconite wt%, Fe, K and Mg content are strongly correlated ($p < 0.001$). Iron mainly present in the sand in the glauconite minerals followed by Fe-oxyhydroxides and pyrite. The variation in Fe content is limited over the different formations and solely linked to the glauconite content. There is no correlation between the Fe^{2+}/Fe_{tot} ratio and any of the studied parameters. The Fe^{2+}/Fe_{tot} ratio is sensitive to oxidation or reduction. Over all samples the ratio ranges between 1/5 – 1/6 though oxidation after sampling could have occurred giving all samples a similar value. The correlations found in the complete sand reflect mostly the glauconite content. No conclusions can be made on the influence of the weathering state of the glauconite as there is no correlation between the glauconite fraction K, Fe and Mg and any of the other investigated parameters.

*Table 4 The correlation coefficients among the properties (GL=glauconite content, total clay content, ratio Fe2+ to Fetot and wt% Fe, K and Mg) of complete glauconite sands and their glauconite fractions and with the distribution coefficient Kd (L/kg) of the complete sand: *** p<0.001; ** p<0.01 and * p<0.05.*

						Complete sand			Glauconite fraction			
		K_d	GL	total clay	$\frac{Fe^{2+}}{Fe_{tot}}$	Fe	K	Mg	Fe	K	Mg	CEC
sand	K_d	1	**0.82****	**0.88****	-0.81	0.64	**0.74***	**0.78***	0.33	0.62	0.53	**0.95*****
	GL%		1	**0.97*****	-0.63	**0.95*****	**0.90****	**0.93*****	0.30	0.42	0.14	**0.82****
	total clay %			1	-0.63	**0.92*****	**0.94*****	**0.97*****	0.31	0.45	0.23	**0.90*****
	$\frac{Fe^{2+}}{Fe_{tot}}$				1	-0.42	-0.37	-0.46	-0.37	-0.44	-0.46	-0.77
	Fe					1	**0.93*****	**0.95*****	0.31	0.30	-0.02	**0.71***
	K						1	**0.99*****	0.32	0.41	0.13	**0.81****
	Mg							1	0.31	0.39	0.14	**0.84****
GL	Fe								1	**0.87****	**0.74***	0.36
	K									1	**0.89****	0.57
	Mg										1	0.44
	CEC											1

The relevant correlations for the K_d are the glauconite content, the total clay content, the K and Mg content of the complete sand and the CEC. The correlation between the Cs K_d and total K in the complete sands is significant and positive (r=0.74), but not between the K_d and the K of the glauconite fraction. Several studies found strong positive associations between total K of clay fractions or soils and the K_d (de Preter 1990, Waegeneers et al. 1999, Uematsu 2017). In sand-clay mixtures and soils, the total K content will often relate to the illite content. Compared to mica and kaolinite, illite has both higher interlayer K and more FES, resulting in higher Cs K_d values. In pure illite like clays, e.g. glauconite, the amount of interlayer K is much higher than the amount of exchangeable K explaining the absence of correlation to the K_d. Not surprisingly, K_d values also rise with increasing XRD detected clay (r= 0.90) and increasing glauconite content (r=0.82). The CEC is here a good predictor of the sorption potential (r=0.95), even though the frayed edges sites, constitute only a small fraction of the total CEC (~ 0.25 % (Bradbury & Baeyens, 2000)). If more smectite and mica type clays would be present the ratio FES to CEC would decrease. In that case the CEC is a less accurate predictor of the radiocesium interception potential.

The regression analysis suggests that the K_d of the glauconite sand can be predicted based on the glauconite content of the sand (r=0.82, p<0.01). Therefore a small test was set up. For four samples the K_d was determined

for the complete sand and its glauconite fraction (Table 5). Based on the glauconite content and the K_d of the isolated glauconite fraction, the K_d of the complete sand can be estimated. This assumes that glauconite is the main sorbing component. In samples where glauconite makes up almost the complete clay mineral fraction, this assumption is valid. In the Voort Formation V3 sample, the true clay size fractions increases towards the Boom Clay Formation. In these samples a prediction based on the glauconite underestimates the K_d of the complete sand showing that the glauconite is not the only reactive clay in the intact sand. The other reactive minerals in the Voort samples are smectite, illite-smectite mixed layer, kaolinite and muscovite. The ratio glauconite to total clay is > 0.84 for all samples of the Diest and Berchem Formation. In the Voort Fm the glauconite to total clay ratio is 0.48-0.59. The hypothesis is that for the Voort Fm samples the smectite and illite-smectite will sorb a significant part of the Cs.

3.3 Effect of the K concentration in the pore water – In-situ K_d

The Neogene-Paleogene glauconite sands were deposited in marine and estuarine environments in which average K concentrations were about 10 mM upon deposition (Millero et al. 2008). Over time, the salt concentration in the sands evolved due to exchange between the pore water and the groundwater. The concentration of K in current groundwater ranges between 0.14 – 0.37 mM, lower than the 0.5 mM K used in the batch sorption experiments. The aquifer solutions have K concentrations at the high end of the range for standard groundwater, though still in the normal range for pore waters. The in-situ K_d can be approximated by using the $K_d.m_K$ relation and the K concentration of the pore water at the corresponding depth and formation. The log K_d range of 3.4 – 3.9 L kg^{-1} at 0.5 mM K translates in values ranging from 3.7 to 4.2 L kg^{-1} at in-situ concentrations. The lower competition effect implies that the in-situ sorption is expected to be higher than the sorption in the batch experiments at 0.5 mM K.

3.4 Sorption kinetics of Cs in glauconite sands and pellets

The sorption kinetics were followed up for D1, B2, V1 and BC for 253 days (~ 8.5 months) on six replicates. The K_d evolutions with time are shown in Figure 3a. After 48h, ^{137}Cs sorption is already rather strong (log K_d 2.6-3.0), followed by slower sorption, the K_d increases factors 6-8 between 48h and 1 month, with minor changes beyond 1 month. The experiment was repeated for all samples in duplicate (up to 9.5 months) and

showed the same trends as the initial experiment. Hence, the 4-5 days needed for reaching equilibrium in illite suspensions (Poinssot et al. 1999) are far exceeded in these samples. Interestingly, the Boom Clay sample shows the same trend (Figure 3).

For ^{137}Cs sorption on illite, sorption on the FES is considered fast, though slower sorption takes place over months and explains the long-term ageing reactions of ^{137}Cs in soil, also denoted with ecological half-lifes (e.g. 3.5 – 5.6 years (Merz et al. 2016)). This slower sorption process is described as interlayer migration (Fuller et al. 2015). The K_d (at 0.5 mM K) did not significantly rise between 1-2 months, however a rise is detected after 8.5 months: the K_d increased between 1 and 8.5 months by factor 1.7 (D1), 1.8 (B2), 1.6 (V1) and 1.8 (BC).

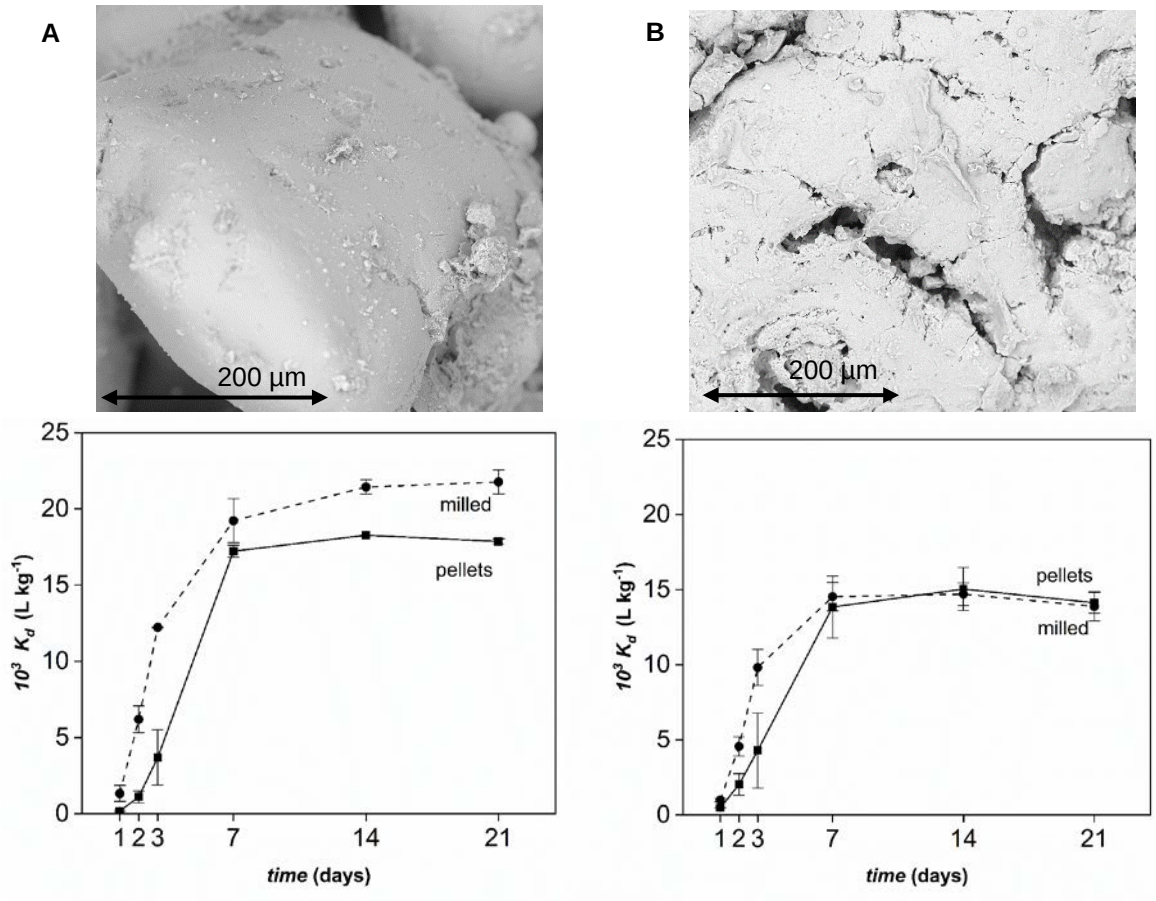

Figure 3 SEM images of the surface of glauconite grains and the evolution of the Kd over time for milled and unmilled glauconite pellets. A) B1 - unweathered Berchem Fm sample b) B6 - strongly weathered surface sample (Berchem Fm).

For the more extended data (up to 9.5 months) of a set of nine glauconite sands the correlation between the K content in the glauconite sand and the change in ^{137}Cs K_d at several time frames is given (Table 6). On the short term sorption reactions there is no significant effect of K content. However, the factor change in ^{137}Cs K_d (> 1

month) is positively correlated with the K content of the sand i.e. there are more slow reactions as the total K over the sands increases. This can be explained by the fact that part of the K that is bound in the interlayer, can be exchanged by Cs over longer time frames.

Table 5 Correlation coefficients r between the potassium content of the glauconite sand and the factor change in 137Cs Kd within various timeframes (for nine glauconite sands).

Time frame	r	p-value
48h/9.5m	-0.56	0.12
16d/9.5m	-0.64	0.06
1m/9.5m	-0.71	0.03*
2m/9.5m	-0.70	0.03*

The glauconite in the Neogene-Paleogene sands occurs mainly as pellets of, on average, ~150 µm. The size and density of the pellets can restrict the access of ^{137}Cs to the FES at the interior of the pellet. The sorption on the pellets is obviously most environmentally relevant. However, due to weathering, fractures can form in the pellet surface or the pellets can disintegrate to clay particles. A comparison of the sorption kinetics between milled (grain size > 2 µm) and unmilled pellets was made in a batch sorption experiment on five glauconite sands and two glauconite fractions.

Milled samples sorb ^{137}Cs faster and more Cs compared to the equivalent unmilled sample (Table 7). In the first 48 hours, the milled samples reacted faster than the glauconite pellets indicating reduced access to the sorption sites. The ratio milled to unmilled glauconite fraction K_d stabilized after 7 days. Beyond 7 days the K_d is 1.1-1.6 times larger for milled than for unmilled samples. This means that part of the inner sorption sites of the pellets remain inaccessible for ^{137}Cs sorption. Our set contains one exception, B6-GL, a heavily weathered Diest Formation sample. Though the milled fraction responded faster than the pellets, the equilibrium K_d is the same (Figure 4). In the weathered sample, the glauconite grain surface is cracked and highly porous as shown in the SEM picture. We assume that the inner pellet sorption sites become accessible for Cs due to the cracks in the outer surface.

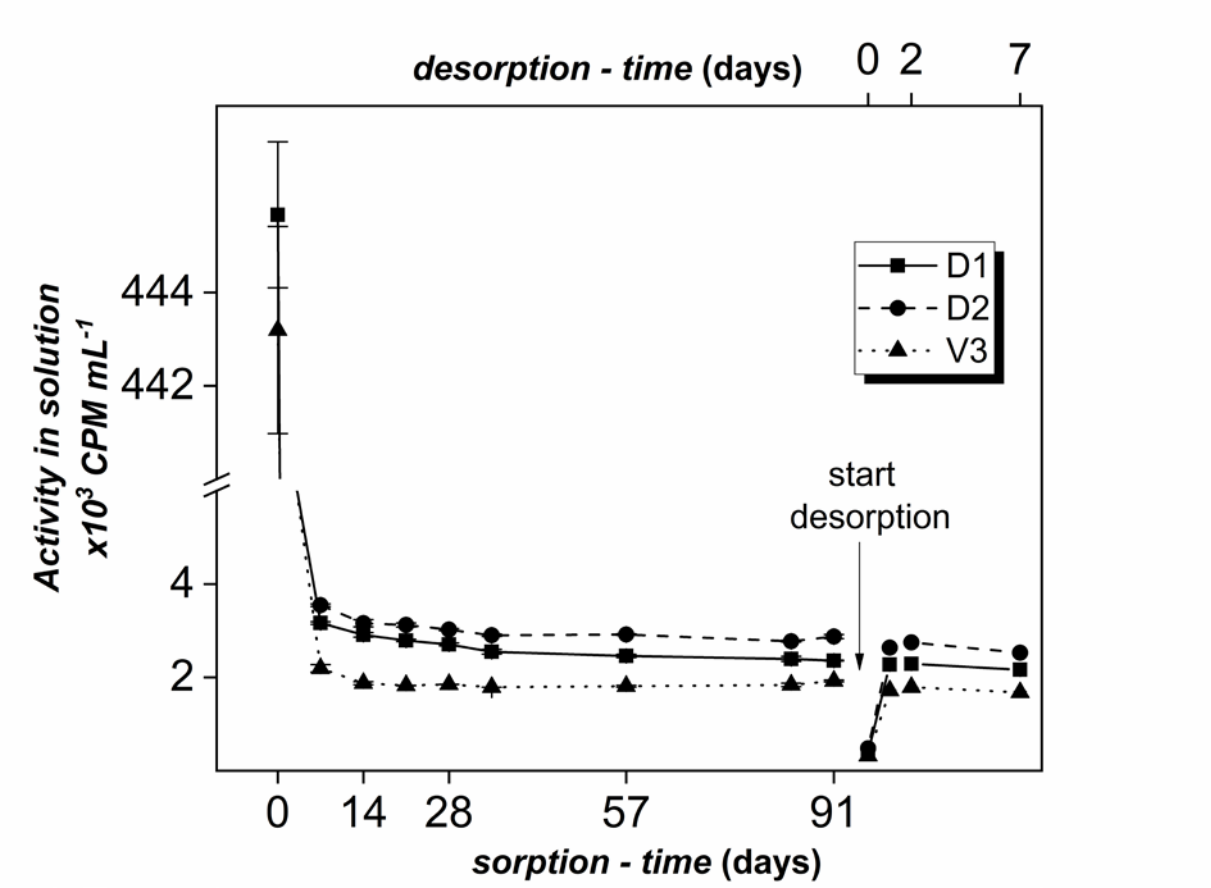

Figure 3 The activity in solution (CPM mL-1) versus time for sorption and desorption. Desorption reaches equilibrium after 2 days. The activity in solution after desorption is only 0.87-0.92 of the corresponding activity in solution after adsorption at 91 days (table 8).

3.5 Adsorption-desorption of ^{137}Cs in glauconite sands

Adsorption-desorption experiments were performed to test reversibility of sorption. The desorption phase used the same concentration of K and Ca as in the adsorption phase, i.e. mimicking the release of Cs under natural pore water concentrations. In Figure 4 the activity in solution is plotted during sorption and desorption for three complete glauconite sands (D1, D2 and V3). The complete glauconite sands reach desorption equilibrium after 2 days, in the milled samples only one day is required. If the sorption is fully reversible, the activity concentration in solution at desorption equilibrium, corrected for dilution, is identical to that of sorption at sorption equilibrium. For example, for sample D2 the activity in the adsorption solution after 3 months was 2873 ± 44 CPM mL^{-1}. After correcting for the activity removed from solution a new solution activity concentration of 2869 CPM mL^{-1} was calculated. The activity concentration at desorption equilibrium was 2529 ± 9 CPM mL^{-1}, i.e. a fraction 0.88 of the corresponding value after adsorption. This indicates some sorption irreversibility. For all investigated glauconite sands, these fractions ranged 0.73-0.95 depending on the sample (Table 8). Additionally,

this fraction is smaller (higher retention) in milled than in unmilled glauconite sands. This implies that milling the sample does not only increase the sorption potential of the glauconite sand, but also the sorption retention.

Table 8. the activity in solution (As) at equilibrium (CPM mL-1) , 3 months for sorption, 7 days for desorption. Several fractions were used in the experiment: complete glauconite sand (C), milled glauconite sand (M), glauconite fraction (GL) and milled glauconite fraction (GLM). The ratio is calculated by dividing the As at desorption equilibrium by the As at sorption equilibrium. A value of 0.99 would indicate reversible Cs sorption, everything below indicates Cs retention.

sample	fraction	Sorption	Desorption	Ratio
		CPM mL^{-1}	CPM mL^{-1}	
B2	C	1581 ± 142	1499 ± 37	0.95
	M	1441 ± 65	1289 ± 13	0.89
D1	C	2360 ± 10	2167 ± 43	0.92
	M	1773 ± 102	1560 ± 19	0.88
V1	C	2044 ± 261	1774 ± 30	0.87
D2	C	2873 ± 44	2529 ± 9	0.88
	M	2598 ± 387	2023 ± 81	0.78
V2	C	2563 ± 168	2418 ± 8	0.94
D3	C	3180 ± 409	2941 ± 24	0.92
D4	C	2710 ±58	2426 ± 18	0.89
D5	C	1373 ± 70	1158 ±3	0.84
B1	C	740 ± 50	713 ± 5	0.96
	GL	729 ± 65	622 ± 3	0.85
	M	745 ± 12	611 ± 8	0.82
V3	C	1923 ± 19	1678 ± 25	0.87
	M	1425 ± 74	1220 ± 19	0.86
	GL	758 ± 12	670 ± 17	0.88
B3	GL	1540 ± 9	1126 ± 1	0.73
IDP		851 ± 12	807 ± 6	0.77

4 Conclusion

This study showed that glauconite sands have strong radiocaesium sorption potential, the log K_d (L kg^{-1}) at 0.5 mM K ranged 3.4 – 4.3 with a limited variation in the sorption potentials among the investigated sands despite the natural diversity of the sand. The in-situ radiocaesium sorption can be expected to be even higher (3.7 – 4.2 log K_d) due to lower K concentrations in the aquifer solutions (less competition effect). The sorption potential of a glauconite sand can be estimated from its percentage glauconite content, in case that the fraction of other clays is low. Comparing milled versus unmilled glauconite, sorption data indicate that part of the inner pellet is not accessible for ^{137}Cs. This effect is not present in weathered glauconite grains as cracks in the grain surface open

up allowing access for ^{137}Cs. In the unweathered samples, the grain size effects (assessed by the comparison of milled versus unmilled samples) are still limited with respect to the range of sorption potentials over all sands. Cs sorption is not fully reversible on the glauconite sands in natural pore water concentrations. In addition, ^{137}Cs sorption kinetics on glauconite sands showed slower reaction than that estimated earlier in soils or clay fractions. We speculate that these slow reactions are likely important for reactive transport of Cs sorption in the high permeable sands where the local non-equilibrium may induce early breakthrough. Such requires further column transport studies.

Acknowledgements

This study is performed in the framework of a PhD in close cooperation with, and with financial support of ONDRAF/NIRAS, the Belgian Agency for Radioactive Waste and Fissile Materials. The authors thank EIG EURIDICE for providing the samples.

References

Adriaens R, Vandenberghe N, Elsen J. Natural clay-sized glauconite in the neogene deposits of the Campine Basin (Belgium). Clays and Clay Minerals 2014; 62: 35-52.

Bradbury MH, Baeyens B. A generalised sorption model for the concentration dependent uptake of caesium by argillaceous rocks. Journal of Contaminant Hydrology 2000; 42: 141-163.

Comans RN, Haller M, De Preter P. Sorption of cesium on illite: non-equilibrium behaviour and reversibility. Geochimica et Cosmochimica Acta 1991; 55: 433-440.

Courbe C, Velde B, Meunier A. Weathering of glauconites: reversal of the glauconitization process in a soil profile in western France. Clay Minerals 1981; 16: 231-243.

Cremer M, Schlocker J. Lithium borate decomposition of rocks, minerals, and ores. American Mineralogist 1976; 61: 318-321.

de Preter P. Radiocesium retention in the aquatic, terrestrial and urban environment: a quantitative and unifying analysis. 1990.

Fritz SF, Popp RK. A single-dissolution technique for determining FeO and Fe_2O_3 in rock and mineral samples. American Mineralogist 1985; 70: 961-968.

Fuller AJ, Shaw S, Peacock CL, Trivedi D, Small JS, Abrahamsen LG, et al. Ionic strength and pH dependent multi-site sorption of Cs onto a micaceous aquifer sediment. Applied Geochemistry 2014; 40: 32-42.

Fuller AJ, Shaw S, Ward MB, Haigh SJ, Mosselmans JFW, Peacock CL, et al. Caesium incorporation and retention in illite interlayers. Applied Clay Science 2015; 108: 128-134.

Merz S, Shozugawa K, Steinhauser G. Effective and ecological half-lives of 90Sr and 137Cs observed in wheat and rice in Japan. Journal of Radioanalytical and Nuclear Chemistry 2016; 307: 1807-1810.

Meunier A, El Albani A. The glauconite?Fe-illite?Fe-smectite problem: a critical review. Terra Nova 2007; 19: 95-104.

Millero FJ, Feistel R, Wright DG, McDougall TJ. The composition of standard seawater and the definition of the Reference-Composition Salinity Scale. Deep Sea Research Part I: Oceanographic Research Papers 2008; 55: 50-72.

Missana T, García-Gutiérrez M, Benedicto A, Ayora C, De-Pourcq K. Modelling of Cs sorption in natural mixed-clays and the effects of ion competition. Applied Geochemistry 2014; 49: 95-102.

Odin G. Green marine clays. Developments in Sedimentology 1988; 45: 1-444.

Poinssot C, Baeyens B, Bradbury MH. Experimental and modelling studies of caesium sorption on illite. Geochimica Et Cosmochimica Acta 1999a; 63: 3217-3227.

Poinssot C, Baeyens B, Bradbury MH. Experimental Studies of Cs, Sr, Ni and Eu sorption on Na-illite and the modelling of Cs sorption. Paul Scherrer Institut (PSI), Villigen, 1999b.

Sawhney B. Selective sorption and fixation of cations by clay minerals: a review. Clays Clay Miner 1972; 20.

Shapiro L. A spectrophotometric method for the determination of FeO in rocks. US Geol. Surv. Profess. Papers 1960; 400: 496-497.

Środoń J, Drits VA, McCarty DK, Hsieh JC, Eberl DD. Quantitative X-ray diffraction analysis of clay-bearing rocks from random preparations. Clays and Clay Minerals 2001 49: 514-528.

Suhr NH, Ingamells CO. Solution Technique for the Analysis of Silicates. Analytical Chemistry 1966; 38: 730-734.

Takeno N. Atlas of Eh-pH diagrams. Geological survey of Japan open file report 2005; 419: 102.

Uematsu S, Smolders E, Sweeck L, Wannijn J, Van Hees M, Vandenhove H. Predicting radiocaesium sorption characteristics with soil chemical properties for Japanese soils. The Science of the Total Environment 2015; 524-525: 148.

Uematsu S, Smolders E, Vandenhove H, Sweeck L. Radiocaesium transfer to crops in the Fukushima affected environments: a soil chemical and plant physiological approach 2017-03. Biosphere Impact Studies, Environment, Health and Safety, KUL - Katholieke Universiteit Leuven - Division of Soil and Water Management. Doctor of Science. KULeuven, Leuven, Belgium, 2017, pp. 160.

Van Ranst E, De Coninck F. Evolution of glauconite in imperfectly drained sandy soils of the Belgian Campine. Journal of Plant Nutrition and Soil Science 1983; 146: 415-426.

Voronina AV, Blinova MO, Semenishchev VS, Gupta DK. Returning land contaminated as a result of radiation accidents to farming use. J Environ Radioact 2015; 144: 103-12.

Waegeneers N, Smolders E, Merckx R. A statistical approach for estimating the radiocesium interception potential of soils. Journal of Environmental Quality 1999; 28: 1005.

Wauters J, Elsen A, Cremers A, Konoplev A, Bulgakov A, Comans R. Prediction of solid/liquid distribution coefficients of radiocaesium in soils and sediments. Part one: a simplified procedure for the solid phase characterisation. Applied Geochemistry 1996a; 11: 589-594.

Wauters J, Vidal M, Elsen A, Cremers A. Prediction of solid/liquid distribution coefficients of radiocaesium in soils and sediments. Part two: a new procedure for solid phase speciation of radiocaesium. Applied geochemistry 1996b; 11: 595-599.